Formation and Properties of Anchored Polymers with a Gradual Variation of Grafting Densities on Flat Substrates

Tao Wu,[†] Kirill Efimenko,[†] Petr Vlček,[‡] Vladimír Šubr,[§] and Jan Genzer*[,†]

Department of Chemical Engineering, North Carolina State University, Raleigh, North Carolina 27695-7905, Department of Controlled Polymerizations, Institute of Macromolecular Chemistry, Academy of Sciences of the Czech Republic, 162 06 Prague, Czech Republic, and Department of Biomedicinal Polymers, Institute of Macromolecular Chemistry, Academy of Sciences of the Czech Republic, 162 06 Prague, Czech Republic

Received October 7, 2002; Revised Manuscript Received January 27, 2003

ABSTRACT: We show that assemblies comprising anchored polymers with a gradual variation of grafting densities on solid substrates can be generated by first covering the substrate with a molecular gradient of the polymerization initiator, followed by polymerization from the substrate-bound initiator centers ("grafting from"). We apply this technique to prepare grafting density gradients of poly(acrylamide) (PAAm) on flat silica substrates. We demonstrate that using the grafting density gradient geometry, the mushroom-to-brush transition can be accessed on a single sample. This transition is detected by monitoring the dependence of the thickness of the grafted PAAm in a good solvent using variable angle spectroscopic ellipsometry. Wettability experiments performed on the gradient PAAm substrate provide complementary information about the nature of the mushroom-to-brush transition.

Introduction

Recent advances in the field of self-assembly have led to the development of a plethora of new technologies based on soft lithography[1] that enable alternative ways of fabricating two- and three-dimensional patterns on material surfaces. Most soft lithography techniques are based on selective deposition of self-assembled monolayers (SAMs).[2] Various structural patterns with dimensions ranging from hundreds of nanometers to several micrometers are created on the material surface using a "pattern-transfer element" or stamp that has a three-dimensional structure molded onto its surface. Because of the molecular nature of the SAMs, the surface patterns generated via soft lithography are rather thin; their thicknesses range from several angstroms to several nanometers. However, some applications, particularly those involving subsequent microfabrication steps, such as etching, require that thicker layers of the surface coating be formed. To accomplish this, techniques, involving the patterning of thicker polymer layers grafted to the substrate, have been developed.[3−9] The latter group of technologies is based on selectively decorating the material surfaces with polymerization initiators and then performing the polymerization directly on the surface ("grafting from"). Using this methodology, the thickness of the overcoat film can be adjusted by simply varying the polymerization conditions (i.e., time, monomer concentration, temperature).

The soft-lithography techniques always produce sharp boundaries between the distinct chemical regions on the substrate. This feature is useful for creating substrates with well-defined chemical patterns of various shapes and dimensions. However, for some applications, it is desirable that the physicochemical characteristics, such as wetting of the substrate, change gradually. The latter can be accomplished by producing surfaces with a position-dependent and gradually varying chemistry. In these so-called "gradient surfaces", the gradient in surface energy is responsible for a position-bound variation in physical properties, most notably the wettability.[10] Recent studies have reported on the preparation of molecular gradients on length scales ranging from nanometers to centimeters.[11,12]

All gradient techniques presented to date led to the formation of two-dimensional gradient patterns. As mentioned earlier, manufacture of miniature devices and applications in lithography often requires the formation of three-dimensional structures. By combining the method of preparing molecular gradients on solid flat substrates with the surface-initiated polymerization, we have recently prepared surface anchored polymers with gradually varying grafting densities.[13] We have shown that such structures can be successfully used to study the mushroom-to-brush transitions. The goal of this paper is to provide more details on the preparation of such structures and demonstrate the general versatility of this novel assembling technique.

Experiment

We formed gradient of polymerization initiator on silica substrates using the methodology proposed by Chaudhury and Whitesides.[10] Specifically, 1-trichlorosilyl-2-(m/*p*-chloromethyl phenyl) ethane (CMPE) (United Chemical Technologies, Inc.) was mixed with paraffin oil (PO), and the mixture was heated to 88 °C and placed in an open container that was positioned close to an edge of a silicon wafer. As CMPE evaporated, it diffused in the vapor phase and generated a concentration gradient along the silica substrate. Upon impinging on the substrate, the CMPE molecules reacted with the substrate −OH functionalities and formed a self-assembled monolayer (SAM). The breadth and position of the CMPE molecular

* To whom correspondence should be addressed: Tel.: +1−919-515-2069, Email: Jan_Genzer@ncsu.edu.
[†] North Carolina State University.
[‡] Department of Controlled Polymerizations, Institute of Macromolecular Chemistry, Academy of Sciences of the Czech Republic.
[§] Department of Biomedicinal Polymers, Institute of Macromolecular Chemistry, Academy of Sciences of the Czech Republic.

10.1021/ma0257189 CCC: $25.00
Published on Web 03/05/2003

gradient can be tuned by varying the CMPE diffusion time and the flux of the CMPE molecules. The latter can be conveniently adjusted by varying the CMPE:PO ratio and the temperature of the diffusing source. To minimize any physisorption of monomer and/or the polymer formed in solution on the parts of the substrate that do not contain the CMPE-SAM, we backfilled the unexposed regions on the substrate (containing unreacted −OH functionalities) with *n*-octyl trichlorosilane, (OTS) (Gelest, Inc.). After the OTS−SAM deposition, any physisorbed CMPE and OTS molecules were removed by thoroughly washing the substrates with warm deionized (DI) water (75 °C, resistivity > 16 MΩ·m) for several minutes. The polymerization of acrylamide was performed by atom transfer radial polymerization (ATRP), as described earlier[14−16] by placing the samples into 120 mL of *N*,*N*′-dimethylformamide and by adding 0.3 g of CuCl, 1.0 g of bipyridine, and 24.0 g of acrylamide (all obtained from Aldrich and used as received). The flask was sealed under N_2 and placed into an oil bath, and the mixture was reacted at 130 °C for controlled time to form PAAm brushes on silica substrates. After the reaction, any physisorbed monomeric and poly(acrylamide) (PAAm) was removed by Soxhlet extraction with DI water for 48 h and dried with nitrogen. In addition, PAAm brushes were grown on silica gels (Davisil, grade 645, surface area ≈ 300 m^2/g) using the procedure outlined in ref 15. The PAAm polymers were grown and purified using the same conditions as described above. The PAAm chains were then cleaved from the silica support with a 10% (w/w) solution of HF for 2 h, neutralized by adding sodium carbonate, and filtered. We note that in addition to the grafted PAAm, free PAAm was also formed in solution.[17] The latter polymers were brown-green colored due to contamination with the residual initiating system. They were dissolved in water and purified by passing through 20 cm column with alumina (aluminum oxide for chromatography, Fluka) and then precipitated into 20-fold excess of acetone. The obtained polymers in form of white or yellowish powder were filtered, washed again with acetone, and dried in vacuo. The molecular weight of PAAm was determined by size exclusion chromatography (SEC) on Superose 12 column (Äkta Explorer, Amersham Bioscience) equipped with differential refractometer and multiangle light scattering detector DAWN DSP-F (Wyatt Technology Corp.). 0.3M sodium acetate buffer (pH ≈ 6.5) was used as the mobile phase. The flow rate was 0.5 mL/min. The molecular weight of the PAAm macromolecules cleaved from the silica gels was M_w = 17 kDa, polydispersity index = 1.7. Huang and Wirth reported a value of M_w = 15.6 kDa for the concentration of monomer, polymerization temperature, and time that were the same as in our experiments.[15] We stress that the molecular weight of the PAAm grown on the silica gels only resembles that of the polymers prepared on the flat substrate because of different steric constrains imposed on the polymers grown in these two different geometries. Nevertheless, we use the molecular weight on the silica gel-grown polymers in our calculations as the best estimate we can currently make. The molecular weight of the solution−polymerized PAAm polymers was found to be consistently 3−5 times that of the cleaved PAAm.[18] In our analysis, we only use the molecular weight determined on the cleaved PAAm.

We used near-edge X-ray absorption fine structure (NEXAFS) to study the chemistry and molecular orientation of the SAMs surfaces.[19] The NEXAFS experiments were carried out on the U7A NIST/Dow Materials Soft X-ray Materials Characterization Facility at the National Synchrotron Light Source at Brookhaven National Laboratory (NSLS BNL). The NEXAFS spectra were collected in the partial electron yield (PEY) at the normal (θ = 90°), grazing (θ = 20°), and so-called "magic" angle (θ = 55°) incidence geometries, where θ is the angle between the sample normal and the polarization vector of the X-ray beam.

The wetting experiments were performed using a Ramé−Hart contact angle goniometer (model 100-00) equipped with a CCD camera, and analyzed with the Ramé−Hart software. The advancing contact angles were read by injecting 6 μL of probing liquid. Each data represents an average over five measurements on the same sample. The data points have an error better than ±1.5°.

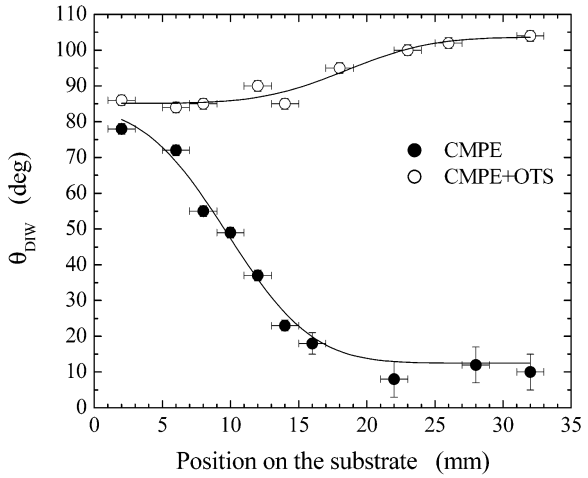

Figure 1. Dependence of the DI water contact angles, θ_{DIW}, on the position along the gradient substrate measured after the CMPE-SAM formation (solid circles) and after backfilling with the OTS-SAM (open circles). The data points have an error of ±1.5 deg and ±1 mm on the vertical and horizontal scales, respectively. The lines are meant to guide the eyes.

The thickness of SAM and the polymer layer was measured using a single-wavelength fixed geometry ellipsometer (AutoEL II, Rudolph Technologies) and a variable angle spectroscopic ellipsometry (J. A. Woollam, Inc.). The thickness was evaluated from the experimentally measured ellipsometric angles Ψ and Δ using the supplied software (DafIMB and WVASE32). The effective indices of refraction of the SAMs and PAAm were taken to be equal to 1.45[2] and 1.54,[20] respectively. The wet thickness of the PAAm in aqueous solutions was measured by placing the samples in a custom-designed solution cell, incubating them for a desired period of time (typically more than 5 h) and performing the experiments with VASE at ϕ = 70°, where ϕ is the angle between the incoming beam and the sample normal. The ellipsometric angles Ψ and Δ were collected for a series of wavelengths ranging from 240 to 1000 nm. The wet PAAm thickness was evaluated using a graded effective medium approximation model based on linear combination of the optical constants of the DI water and PAAm/DI water mixtures. We also attempted to model the VASE data using other models, including a single layer and a multilayer approximations. We found that while the actual values of H deviate slightly (up to 5%), the trends seen are the same, regardless of the model used.

Results

In Figure 1, we plot the variation of the contact angle of deionized (DI) water, θ_{DIW}, as a function of the position on the sample measured on the CMPE-SAM covered substrate (closed circles) and the substrate that was backfilled with the OTS-SAM (open circles). The CMPE source (CMPE:OTS ratio = 1:1 (w/w)) was allowed to diffuse for 2 min at 88 °C; the OTS-SAM was generated by exposing the substrate to OTS vapor for 15 min at room temperature. The data in Figure 1 show that the contact angle of CMPE decreases gradually from ≈78° down to ≈0° as one moves across the substrate starting at the CMPE side. After the OTS deposition, the regions on the substrate far from the diffusing source are covered with a complete monolayer of OTS (contact angle ≈100°). As one traverses across the CMPE gradient, the contact angle decreases from ≈100° (OTS side) down to ≈86° (CMPE side). The minute increase of the contact angle within the CMPE-SAM is likely a result of small interpenetration of OTS into the CMPE-SAM.

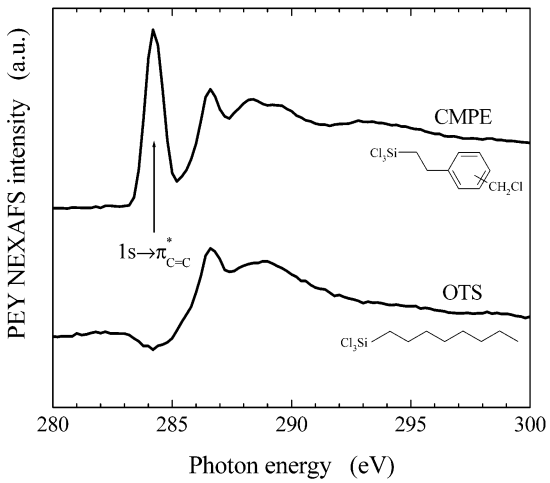

Figure 2. Carbon K-edge PEY NEXAFS spectra collected from the CMPE-SAM (top) and OTS-SAM (bottom). The arrow marks the position of the 1s → π^* transition for phenyl C=C, present only in the CMPE-SAM sample.

NEXAFS spectroscopy was used to provide detailed chemical and structural information about the SAMs on the substrate. In Figure 2, we plot the carbon edge K-edge NEXAFS spectra taken from CMPE-SAM (top) and OTS-SAM (bottom) samples. The NEXAFS spectra collected at the "magic" angle were indistinguishable from those recorded at the normal and grazing incidence geometries. This revealed that the CMPE-SAMs were not oriented, rather they formed a "liquid-like" structure. This observation is in accord with recent reports from the Chaudhury and Allara groups who studied the transitions between the "liquid-like" and "semicrystalline-like" structures in hydrocarbon SAMs.[21] The NEXAFS spectra in Figure 2 both contain peaks at 286.0 and 288.5 eV that correspond to the 1s → σ^* transition for the C−H and C−C bonds, respectively. In addition, the spectrum of CMPE also exhibits a very strong signal at 284.2 eV, which can be attributed to the 1s → π^* transition for phenyl C=C.[19] The latter signal can thus be used as an unambiguous signature of CMPE in the sample. With the X-ray monochromator set to 284.2 eV, we collected the PEY NEXAFS signal by scanning the X-ray beam across the gradient.[22] The lines in Figure 3 show the variation of the PEY NEXAFS intensity measured at 284.2 eV across the gradient samples prepared by diffusing CMPE for 2 min from mixtures with various CMPE:PO ratios equal to 1:1 (solid line), 1:2 (dashed line), 1:5 (dotted line), and 1:10 (dash−dotted line). In the remainder of the paper, we refer to such substrates as S1, S2, S5, and S10, respectively. The data in Figure 3 reveal that the NEXAFS intensity from the C=C phenyl bond, and thus the concentration of CMPE in the sample, decreases as one moves from the CMPE side of the sample toward the OTS-SAM; the functional form closely resembles that of a diffusion-like profile. Moreover, the concentration within each gradient can be fine-tuned by varying the CMPE:PO ratio. Experiments using VASE confirmed that only a single monolayer was formed along the CMPE gradient substrate.

After the preparation of the CMPE-gradient substrate, the ATRP polymerization of PAAm was performed as described previously. VASE and AutoEL II were used to measure the thickness of the dry polymer film, h, as a function of the position on the substrate. In Figure 4 we plot the values of h for samples prepared

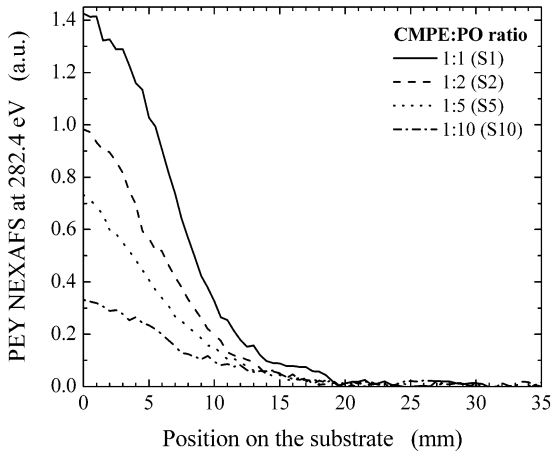

Figure 3. PEY NEXAFS intensity measured at E = 284.2 eV as a function of the position the substrates containing the initiator gradients made of CMPE:OTS mixtures (w/w) 1:1 (solid line), 1:2 (dashed line), 1:5 (dotted line), and 1:10 (dash−dotted line).

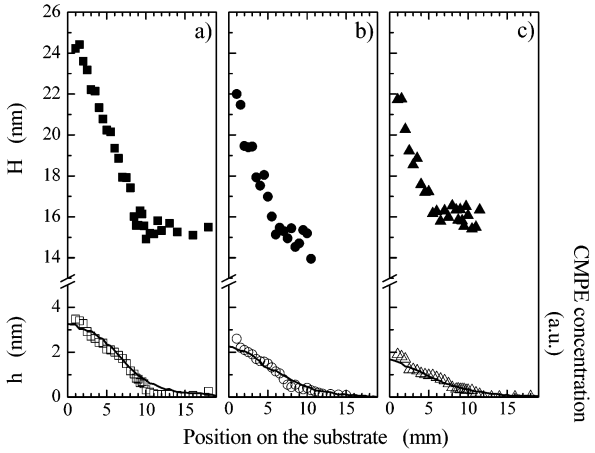

Figure 4. Dry thickness, h (open symbols), and wet thickness, H (closed symbols), of PAAm and the CMPE concentration (solid line) as a function of the position on the substrate for samples prepared on substrates containing the initiator gradients made of CMPE:OTS mixtures (w/w): (a) 1:1 (squares), (b) 1:2 (circles), and (c) 1:5 (triangles).

on the (a) S1 (open squares), (b) S2 (open circles), and (c) S5 (open triangles) substrates. From Figure 4, h decreases gradually as one moves across the substrate starting at the CMPE edge. Note the agreement between the variation of h and the concentration profiles of the CMPE initiator (solid lines). Because the polymers grafted on the substrate all have roughly the same degree of polymerization (see discussion below), the variation of the polymer film thickness can be attributed to the difference in the density, σ, of the CMPE grafting points on the substrate. The grafting density can be calculated from $\sigma = h\rho N_A/M_n$, where ρ is the density of PAAm (=1.302 g/cm^3), N_A is Avogadro's number, and M_n is the polymer molecular weight.

The substrates with the grafted PAAm were placed into a solution cell that was filled with DI water (pH ≈ 7), a good solvent for PAAm, and incubated for at least 5 h. The wet thickness of PAAm grafted polymer in DI water, H, was measured using VASE. The top parts of Figure 4 shows the values of H for samples prepared on the (a) S1 (closed squares), (b) S2 (closed circles), and (c) S5 (closed triangles) substrates. The data show that in all cases H decreases as one traverses across the

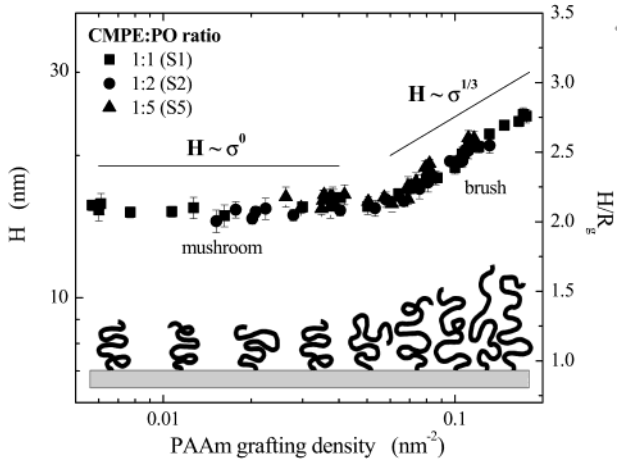

Figure 5. Wet thickness of PAAm as a function of the PAAm grafting density for samples prepared on substrates containing the initiator gradients made of CMPE:OTS mixtures (w/w) 1:1 (squares), 1:2 (circles), and 1:5 (triangles). The inset shows a cartoon illustrating the polymer behavior.

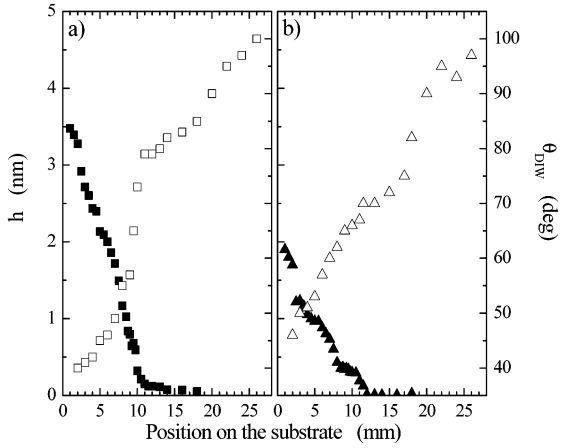

Figure 6. Dry thickness of PAAm, h, (closed symbols) and contact angle of DI water, θ_{DIW}, (open symbols) as a function of the position on the substrate for samples prepared on substrates containing the initiator gradients made of CMPE:OTS mixtures (w/w) 1:1: (a) (squares) and (b) 1:5 (triangles). The contact angle data have an error better than ±1.5° and ±1 mm on the vertical and horizontal scales, respectively.

substrate stating at the CMPE side. The maximum brush height at the CMPE edge of the sample decreases with decreasing CMPE concentration on the substrate (S1 > S2 > S5).

Discussion

We have established that the grafting density of end-anchored polymers on surfaces can be conveniently adjusted by first creating a gradient density of the surface-bound initiator followed by "grafting-from" polymerization. Our analysis presented in the previous section showed that the concentration of the CMPE polymerization initiator varied gradually across the substrate. The gradient profile width measured by NEXAFS was in accord with that obtained from the position-dependent contact angle data (cf. Figure 1). We have also shown that the concentration of the CMPE molecules within the gradient can be fine-tuned by varying the CMPE:PO ratio. We note that the width of the gradient (and its position on the substrate) can also be adjusted by varying the diffusion time or/and the temperature of the CMPE:PO diffusing source. For each sample studied, the dry PAAm thickness profile as a function of the position on the substrate coincides with the concentration profile of the CMPE initiator (cf. Figure 3). This agreement demonstrates that the initiator molecules are firmly bonded to the substrate and that they do not desorb from the substrate during the polymerization.

In Figure 5, we plot the wet polymer thickness as a function of the PAAm grafting density on the S1 (squares), S2 (circles), S5 (triangles) substrates. The results in Figure 5 demonstrate that at low σ, H is independent of the grafting density. Hence, the surface anchored PAAm chains are in the mushroom regime. At high polymer grafting densities, H increases with increasing σ, which is a signature of the brush behavior. The crossover between the two regimes occurs at $\sigma \approx 0.065$ nm^{-2}. We note that recent publications reported that the crossover region is rather broad.[23,24] We will return to this point later in the paper. By fitting the data in the brush regime to $H \sim N\sigma^n$ we obtain n equal to 0.37 ± 0.04 (S1 substrate), 0.39 ± 0.05 (S2 substrate), and 0.40 ± 0.06 (S5 substrate). We note that n obtained by fitting the experimental data is slightly higher that the predicted value of $n = {}^1/_3$; this observation is in agreement with recent reports.[25] A remark has to be made about the possible variation of the chain length with grafting density. Jones and co-workers recently reported on studies of grafting from polymerization of poly(methyl methacrylate) using ATRP from substrates having various surface densities of the polymerization initiator, ω-mercaptoundecyl bromoisobutyrate.[26] Their study revealed that the grafting density of the polymer depends on the grafting density of the initiator. However, on the basis of the data presented in ref 26, it is difficult to discern whether the kinetics of the polymerization also depends on the grafting density of the initiator. Currently we have no means of measuring the molecular weight of the grafted brushes directly on the gradient substrate. While we cannot exclude the possibility that the length PAAm chains polymerized on the various parts of the molecular gradient substrate varies with σ, we note that the fact that the data in Figure 5 superimpose on a single master curve indicates that the polymers have likely very similar lengths, which is not surprising for the rather short anchored polymers synthesized in this work.

In addition to the measurement of the wet brush thickness, we have also performed wettability experiments as a function of the PAAm grafting density on the substrate. Our aim was to corroborate the ellipsometric data and provide more insight into the polymer packing in the surface grafting density gradient. In Figure 6 we plot the dry PAAm thickness, h, (closed symbols) and the contact angles of DI water, θ_{DIW}, (open symbols) as a function of the position on the substrate for samples prepared on the (a) S1 (squares) and (b) S5 (triangles) substrates. In both samples, the dry thickness of PAAm decreases gradually as one moves across the substrate starting at the CMPE edge. The θ_{DIW} values increase as one traverses across the substrate starting at the CMPE side. The increase in θ_{DIW} is not monotonic, it follows a "double S"-type shape. While the "double S"-type dependence of θ_{DIW} on the position on the sample is detected in both S1 and S5 samples, there are differences in the plateau values. Specifically, while for the S1 sample, the three plateaus are located at $\theta_{DIW} \approx 40$, ≈ 83, and $\approx 100°$ the corresponding values for

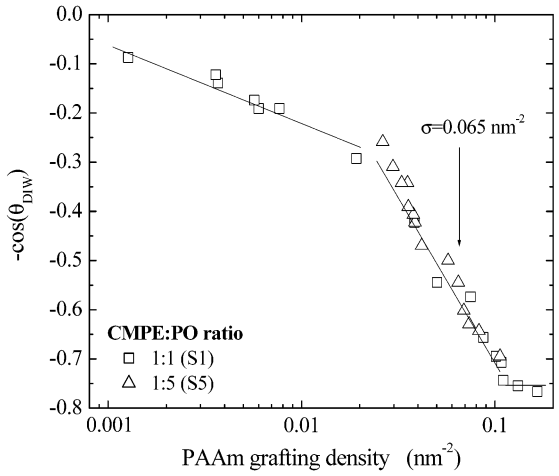

Figure 7. Negative cosine of the contact angle of DI water as a function of the PAAm grafting density on the substrate for samples prepared on substrates containing the initiator gradients made of CMPE:OTS mixtures (w/w) 1:1 (squares) and 1:5 (triangles). The lines are meant to guide the eyes.

the S2 sample are $\theta_{DIW} \approx 47$, ≈ 70, and $\approx 97°$. On the basis of the dry thickness data and our previous discussion, the three plateaus in the contact angle behavior can be attributed to the wetting characteristics inside the brush, mushroom, and OTS (no PAAm) regions. At distances far away from the CMPE edge, where the θ_{DIW} values are high, there is no grafted PAAm on the sample. The contact angle experiments detect the presence of the OTS SAM. By moving closer toward the CMPE edge, the contact angle decreases by $\approx$20−30° indicating that some polymer chains are present on the substrate. However, their grafting densities are low so that the probing liquid can penetrate between the grafted chains; the measured contact angle represents a weighted average between the PAAm and OTS. Upon approaching the mushroom-to-brush transition region, the contact angle further decreases. The decrease is steeper for PAAm on the S1 substrate and more gradual for the S2 sample, indicating that the density of PAAm increases more rapidly in the former case. The contact angles in the lowest plateau are $\theta_{DIW} \approx 40$ and $\approx 47°$ for samples S1 and S5, respectively. In independent experiments we have established that the θ_{DIW} of a pure PAAm is $\approx 37 \pm 2°$.[27] Because in both cases the PAAm polymers grafted on the substrate have roughly the same degree of polymerization, the variation of the polymer film thickness can be attributed to the difference in the density of the CMPE grafting points on the substrate. Specifically, close to the CMPE edge, the PAAm macromolecules form a dense brush on the S1 substrate and a "semidense" brush on the S5 substrate.

The previous discussion revealed that the θ_{DIW} depends on the grafting density of the PAAm chains on the substrate. Earlier, we have shown that the wet thickness of PAAm prepared on substrates with various CMPE concentrations can be collapsed on a single master curve when plotted as H vs σ. One would thus expect that also the wettabilities of the substrates plotted vs the PAAm grafting density should exhibit similar universal behavior. In Figure 7, we plot the negative cosine of θ_{DIW} as a function of the grafting density of PAAm on substrates S1 (squares) and S5 (triangles). As anticipated, the data collapse on a single master curve. A close inspection of the results present in Figure 7 reveals that the data can be divided into three distinct regions. For $\sigma > 0.1$ nm^{-2}, the chains are expected to be in a brush regime − the wettabilities are close to that of pure PAAm ($-\cos(\theta_{DIW}) \approx -0.79$). For $\sigma < 0.02$ nm^{-2}, the PAAm chains form mushroom conformations on the substrate. In this regime, the wettabilities change slightly because the distance between the chains also changes, although they are already loosely separated on the substrate. At grafting densities 0.02 nm^{-2} $< \sigma <$ 0.1 nm^{-2}, the slope of $-\cos(\theta_{DIW})$ changes rather rapidly. The data in Figure 7 show that the position of the mushroom-to-brush crossover determined using the wettability approach is in accord with the ellipsometric measurements (the transition location was established to be at $\sigma \approx 0.065$ nm^{-2}). However, in the former case, the transition region extends over almost 1 order of magnitude in σ, which is broader than the transition region predicted by the H vs σ data, and is in agreement with recent theoretical work on similar systems.[23,28] We speculate that the small difference between the widths of the mushroom-to-brush region inferred from both types of experiments is likely associated with the inaccuracy in H, which was obtained indirectly by the model fitting of the VASE data.

Conclusions

We have described a method leading to the preparation of surface-anchored polymer assemblies, whose grafting density varies gradually as a function of the position on the substrate. Specifically, we have shown that such structures can be fabricated by first generating a molecular gradient of polymerization initiator on the solid substrate and subsequently carrying out "grafting from" polymerization from the substrate-bound initiator centers. In this publication, we used the above technology to prepare poly(acrylamide) (PAAm) assemblies with gradient variation of grafting densities on silica-covered substrates. We have measured the thickness (H) of PAAm in a good solvent as a function of the PAAm grafting density on the substrate (σ). Our measurements revealed that at low grafting densities, the PAAm chains were in the mushroom regime, the values of H were independent of σ. At high grafting densities, H was found to scale as σ^n, where n ranged from 0.37 to 0.40. This exponent was just slightly higher than the value predicted by mean-field theories of polymer brushes ($n = {}^1/_3$). Complementary wetting experiments on the same samples were performed that confirmed the results of the ellipsometry measurements. Moreover, the wettability experiments revealed that the mushroom-to-brush transition spans a broad range of grafting density (about an order of magnitude in σ). Work is in progress to extend the current study to probe the effect of the polymer length and charge on the interfacial properties of the gradient polymer brushes.[29]

Acknowledgment. This research was supported by the National Science Foundation, Grant No. CTS 0209403, The Camille Dreyfus Teacher−Scholar award, and The 3M Non-Tenured Faculty award. The variable angle spectroscopic ellipsometer was purchased with funds awarded to J.G. through the NSF's Instrumentation for Materials Research Program (Grant No. DMR-9975780). The NEXAFS experiments were carried out at the National Synchrotron Light Source, Brookhaven National Laboratory, which is supported by the U.S. Department of Energy, Division of Materials Sciences

and Division of Chemical Sciences. The authors thank Dr. Daniel Fischer (NIST) for his assistance during the course of the NEXAFS experiments.

References and Notes

(1) Xia, Y.; Whitesides, G. M. *Angew. Chem., Int. Ed. Engl.* **1998**, *37*, 550; Xia, Y.; et al. *Chem. Rev.* **1999**, *99*, 1823.
(2) Ulman, A. *An Introduction to Ultrathin Organic Films from Langmuir−Blodgett to Self-Assembly*; Academic Press: New York, 1991.
(3) Husseman, M.; et al. *Angew. Chem., Int. Ed. Engl.* **1999**, *38*, 647.
(4) Shah, R.; et al. *Macromolecules* **2000**, *33*, 597.
(5) Jeon, N. L. *Appl. Phys. Lett.* **1999**, *75*, 4201. Kim, N.; et al. *Macromolecules* **2000**, *33*, 3793.
(6) de Boer, B.; et al. *Macromolecules* **2000**, *33*, 349.
(7) Ghosh, P.; et al. *Macromolecules* **2001**, *34*, 1230.
(8) Jones, D. M.; Huck, W. T. S. *Adv. Mater.* **2001**, *13*, 1256.
(9) Hyun, J.; Chilkoti, A. *Macromolecules* **2001**, *34*, 5644.
(10) Chaudhury, M. K.; Whitesides, G. M. *Science* **1992**, *256*, 1539.
(11) Efimenko, K.; Genzer, J. *Adv. Mater.* **2001**, *13*, 1560.
(12) Fuierer et al., R. R. *Adv. Mater.* **2002**, *14*, 154.
(13) Wu, T.; Efimenko, K.; Genzer, J. *J. Am. Chem. Soc.* **2002**, *124*, 9394.
(14) Huang, X.; Doneski, L. J.; Wirth, M. J. *CHEMTECH* **1998**, *Dec*, 19; *Anal. Chem.* **1998**, *70*, 4023.
(15) Huang, X.; Wirth, M. J. *Macromolecules* **1999**, *32*, 1694.
(16) Wu, T.; Efimenko, K.; Genzer, J. *Macromolecules* **2001**, *34*, 684.
(17) The free polymer in solution can probably be formed by thermal initiation of acrylamide (AAm). This thermally induced polymerization may proceed in a more or less controllable manner as the reverse ATRP (or RATRP) [Xia, J.; Matyjaszewski, K.; *Macromolecules* **1999**, *32*, 5199]. The AAm radical in combination with $CuCl_2$ represents an active form of the RATRP growing center and can be in equilibrium with the dormant form of the center, i.e., the halogenated AAm combined with CuCl: $AAm^{\bullet} + CuCl_2 \rightleftarrows AAm-Cl + CuCl$. Thermally initiated polymerization of methacrylamide monomers has been reported to proceed slowly. However, given the relatively long reaction time used in our study, it may not be completely negligible [Teodorescu, M.; Matyjaszewski, K. *Macromolecules* **1999**, *32*, 4826].
(18) The rather broad distribution of molecular weights of PAAm achieved under different conditions, particularly in solution and in heterogeneous systems, may originate from possible self-termination of the propagation step due to cyclization reactions [Teodorescu, M.; Matyjaszewski, K. *Macromolecules* **1999**, *32*, 4826. Rademacher, J. T.; et al. *Macromolecules* **2000**, *33*, 284]. In such a case, attainable molecular weight of the polymer will depend on the ratio of the rate of polymerization to that of cyclization. One may speculate that because of smaller steric hindrance and higher mobility, the probability of propagation, i.e., the reaction of the active chain-end with a monomer, is higher in solution relative to that in a heterogeneous polymerization involving surface anchored polymers.
(19) Stöhr, J. *NEXAFS Spectroscopy*; Springer-Verlag: Berlin, 1992.
(20) Brandrup, J., Immergut, E. H., Grulke, E. A., Eds. *Polymer handbook* Wiley: New York, 1999.
(21) Chaudhury, M. K.; Owen, M. J. *J. Phys. Chem.* **1993**, *97*, 5722. Allara, D. L.; Parikh, A. N.; Judge, E. *J. Chem. Phys.* **1994**, *100*, 1761.
(22) Genzer, J.; Fischer, D. A.; Efimenko, K. *Appl. Phys. Lett.* **2002**, *82*, 266.
(23) For a recent review see Kent, M. S. *Macromol. Rapid Commun.* **2000**, *21*, 243 and references therein.
(24) Douglas, J. F.; et al. Polymer Brushes: Structure and Dynamics. *Encyclopedia of Materials: Science and Technology*; Elsevier: Amsterdam, 2001; pp 7218−7223.
(25) Wamamoto, S.; et al. *Macromolecules* **2000**, *33*, 5608.
(26) Jones, D. M.; Brown, A. A.; Huck, W. T. S. *Langmuir* **2002**, *18*, 1265.
(27) To measure the contact angle of DI water on pure PAAm, we have grown PAAm from a substrate covered homogeneously with the CMPE initiator. The polymerization conditions were the same as for the sample described in the text. The contact angle was determined using the technique described in the text.
(28) Carignano, M. A.; Szleifer, I. *Macromolecules* **1995**, *28*, 3197. Szleifer, I. *Curr. Opin. Colloid Interface Sci.* **1996**, *1*, 416. Szleifer, I.; Carignano, M. A. *Adv. Chem. Phys.* **1996**, *XCIV*, 165.
(29) Wu, T.; Genzer, J. Work in progress.

MA0257189